

1 **Heterogeneous expression of the SARS-Coronavirus-2 receptor ACE2**
2 **in the human respiratory tract**
3
4 Miguel E. Ortiz Bezara¹, Andrew Thurman², Alejandro A. Pezzulo², Mariah R. Leidinger³, Julia
5 A. Klesney-Tait², Philip H. Karp², Ping Tan², Christine Wohlford-Lenane¹, Paul B. McCray,
6 Jr.^{1*}, David K. Meyerholz^{3*}

7
8 Departments of Pediatrics¹, Internal Medicine², and Pathology³; University of Iowa College of
9 Medicine, University of Iowa, Iowa City, IA USA

10 *Contributed equally

11
12 Correspondence:

13 David K. Meyerholz (david-meyerholz@uiowa.edu)

14 Paul B. McCray, Jr. (paul-mccray@uiowa.edu)

15
16 **Running title:** Expression of ACE2 in the human respiratory tract

17 **Abstract:**

18 *Background:* Zoonotically transmitted coronaviruses are responsible for three disease outbreaks
19 since 2002, including the current COVID-19 pandemic, caused by SARS-CoV-2. Its efficient
20 transmission and range of disease severity raise questions regarding the contributions of virus-
21 receptor interactions. ACE2 is a host ectopeptidase and the receptor for SARS-CoV-2. Numerous
22 reports describe ACE2 mRNA abundance and tissue distribution; however, mRNA abundance is
23 not always representative of protein levels. Currently, there is limited data evaluating ACE2
24 protein and its correlation with other SARS-CoV-2 susceptibility factors.

25 *Materials and methods:* We systematically examined the human upper and lower respiratory
26 tract using single-cell RNA sequencing and immunohistochemistry to determine receptor
27 expression and evaluated its association with risk factors for severe COVID-19.

28 *Findings:* Our results reveal that ACE2 protein is highest within regions of the sinonasal cavity
29 and pulmonary alveoli, sites of presumptive viral transmission and severe disease development,
30 respectively. In the lung parenchyma, ACE2 protein was found on the apical surface of a small
31 subset of alveolar type II cells and colocalized with TMPRSS2, a cofactor for SARS-CoV2
32 entry. ACE2 protein was not increased by pulmonary risk factors for severe COVID-19.

33 Additionally, ACE2 protein was not reduced in children, a demographic with a lower incidence
34 of severe COVID-19.

35 *Interpretation:* These results offer new insights into ACE2 protein localization in the human
36 respiratory tract and its relationship with susceptibility factors to COVID-19.

37 **Key words:** Lung, expression, alveolar type II cells, ciliated cells, immunohistochemistry

38 Abstract word count: 224

39 Body of paper word count: 4141

41 **Research in context:**

42 *Evidence before this study:* Previous studies of ACE2 mRNA transcript abundance in the human
43 respiratory tract have suggested a possible association between ACE2 expression and age, sex,
44 and the presence of comorbidities. However, these studies have provided conflicting results, as
45 well as a lack of protein validation. Previous ACE2 protein studies have been limited by a
46 paucity of lung tissue samples and reports that have produced contradictory results.

47

48 *Added value of this study:* Using a combination of single-cell RNA sequencing and
49 immunohistochemistry, we describe ACE2 expression in the human respiratory tract. Staining
50 protocols were optimized and validated to show consistent apical localization and avoid non-
51 specific staining. We show ACE2 protein is found in subsets of airway cells and is highest within
52 regions of the sinonasal cavity and pulmonary alveoli, sites of presumptive viral transmission
53 and severe disease development for COVID-19, respectively. We show age, sex, and
54 comorbidities do not increase ACE2 protein expression in the human respiratory tract.

55

56 *Implications of all the available evidence:*

57 ACE2 protein abundance does not correlate with risk factors for severe clinical outcomes, but in
58 some cases showed an inversed relationship. Features driving COVID-19 susceptibility and
59 severity are complex, our data suggests factors other than ACE2 protein abundance as important
60 determinants of clinical outcomes.

61 **Introduction:**

62 Angiotensin-converting enzyme 2 (ACE2) is the cellular receptor for both severe acute
63 respiratory syndrome coronavirus (SARS-CoV) and SARS-CoV-2 (1, 2). SARS-CoV caused a
64 pneumonia outbreak in 2002-2003 with a mortality rate of 9.6% and over 800 deaths worldwide
65 (3). SARS-CoV-2 is the etiologic agent of coronavirus disease 2019 (COVID-19) which was first
66 recognized in December 2019 and has now reached pandemic proportions (2, 4). SARS-CoV-2
67 infection can be fatal, with the risk for increased disease severity correlating with advanced age
68 and underlying comorbidities, while children and younger individuals generally have milder
69 disease (5-11). These trends in disease severity could reflect differences in ACE2 distribution
70 and expression in the respiratory tract.

71

72 Previous studies have evaluated ACE2 expression in the respiratory tract. Studies of ACE2
73 mRNA transcript abundance have provided conflicting interpretations, as well as a lack of
74 protein validation (12-19). ACE2 protein studies have been limited by a paucity of lung tissue
75 substrates and reports that have yielded contradictory results (20-23) ([Supplemental Table 1](#)). It
76 is reported that some clinical factors (sex, age, or presence of comorbidities) could influence
77 ACE2 expression in the human lower respiratory tract. The ACE2 gene resides on the X
78 chromosome and therefore could be differentially regulated between males and females due to
79 variable X-inactivation (24). Increased abundance of circulating ACE2 protein is reported to
80 correlate with male sex, advanced age, and chronic comorbidities such as diabetes,
81 cardiovascular disease, and renal disease (reviewed in (25)). Recent single-cell mRNA
82 sequencing (scRNA-seq) studies of respiratory tract cells have reported contradictory evidence

83 regarding the correlation between ACE2 transcript abundance and age, sex, smoking status, and
84 other comorbidities (12-17).

85

86 We investigated the hypothesis that ACE2 drives disease severity in susceptible patient
87 populations through enhanced abundance or distribution in different locations or cell types of the
88 respiratory tract. We reanalyzed publicly available scRNA-seq data from distal lung biopsies
89 (26), nasal brushings, and nasal turbinate samples (27) to evaluate ACE2 transcript abundance in
90 specific cell types. We complemented these analyses with optimized and validated ACE2
91 immunostaining protocols, to corroborate single cell analyses as well as to screen for differences
92 in cellular ACE2 protein in lung tissues derived from a cohort of control and chronic diseased
93 patients.

94 **Materials and methods:**

95

96 **Ethics:**

97 Studies on human tissues were approved by the institutional review board of the University of
98 Iowa (Iowa IRB #199507432). Informed consent was obtained for all the tissues included in the
99 study.

100

101 **Tissues:**

102 Tissues included nasal biopsies (n=3, deidentified and lacked evidence of significant disease or
103 cancer), lung donors (n=29), primary cell cultures (28), and autopsy tissues (control tissues such
104 as small intestine and kidney) that were selected from archival repositories as formalin-fixed
105 paraffin-embedded blocks. All lungs were derived either from living donors at lung transplant or
106 from deceased individuals maintained on life support for organ donation. In either case, lung
107 tissues were routinely harvested according to transplant guidelines to maintain tissue viability.
108 Lungs were surgically resected, placed in chilled media and transported to lab for examination,
109 sample collection and fixation. Lung cases were selected to comprise two case study groups: 1)
110 Chronic disease group was defined as having chronic comorbidities including: asthma,
111 cardiovascular disease, chronic obstructive pulmonary disease, cystic fibrosis, diabetes, and
112 smoking. 2) Control group was defined as lacking these chronic comorbidities and lacking
113 clinical lung disease. The definition of chronic comorbidities was informed by reported
114 independent risk factors for mortality in COVID-19 (8-10). The cumulative cohort included 29
115 cases (15 chronic comorbidities and 14 controls) with a broad range of ages (0·5 – 71 years) and
116 both sexes were represented (13 female and 16 male). For these lungs, if a trachea or bronchus

117 tissue block was available from the same case – these were included as well ([Supplemental Table](#)
118 [2](#)). Bronchioles were observed in most lung sections and were defined as intrapulmonary airways
119 lacking evidence of cartilage or submucosal glands (29). Detailed medical histories other than
120 diagnoses, including medication history, were not available.

121

122 **Immunohistochemistry and immunofluorescence:**

123 All formalin-fixed paraffin-embedded tissues were sectioned (~4 μm) and hydrated through a
124 series of xylene and alcohol baths to water. Immunohistochemical techniques were used for the
125 following markers: angiotensin-converting enzyme 2 (ACE2) (30), surfactant protein C (SP-C)
126 (31), and mucin 5B (MUC5B) (32). For more specifics about the reagents please see
127 [Supplemental Table 3](#).

128

129 The immunostaining protocols for ACE2 were rigorously optimized and validated to avoid
130 nonspecific staining that is commonplace and give confidence in the sensitivity of the protocol
131 and quality of the tissues ([Supplemental Figure 4](#), [Supplemental Table 1](#) and [Supplemental Table](#)
132 [3](#)). We analyzed ACE2 protein expression in human upper and lower respiratory tract by
133 immunohistochemistry ([Supplemental Table 2](#)). Human respiratory tract tissues were scored for
134 ACE2 expression by a masked pathologist, following principles for reproducible tissue scores
135 (17).

136

137 For immunofluorescence, formalin-fixed and paraffin-embedded human lung blocks were
138 sectioned (~4 μm). Slides were baked (55°C x 15 min) and then deparaffinized (hydrated) in a
139 series of xylene and progressive alcohol baths. Antigen retrieval was performed using Antigen

140 Unmasking Solution (1:100, #H-3300) in citrate buffer (pH 6.0) solution to induce epitope
141 retrieval (5 min x 3 times) in the microwave. Slides were washed (PBS, 3 times, 5 min each) and
142 a PAP pen used to encircle the tissue. Slides were blocked with background blocking solution
143 (2% BSA in Superblock 1 hr in humid chamber). Primary antibodies anti-ACE2 (1:100, Mouse
144 monoclonal, MAB933, R&D Systems, Minneapolis, MN USA) and anti-TMPRSS2 (1:200,
145 Rabbit monoclonal, #ab92323, Abcam, Cambridge, MA USA) were diluted in blocking solution
146 (2% BSA in Superblock overnight 4°C). Secondary antibodies anti-mouse Alexa568 (for ACE2)
147 and anti-rabbit Alexa488 (for TMPRSS2) were applied at a concentration of 1:600 for 1 hour at
148 room temperature. Slides were washed and mounted with Vectashield containing DAPI.

149

150 **Tissue scoring:**

151 Stained tissue sections were examined for ACE2 localization using a post-examination method
152 for masking and scored by a masked pathologist following principles for reproducible tissue
153 scores (33). The initial examination showed a low heterogenous incidence of ACE2 staining for
154 various tissues, so the following ordinal scoring system was employed to quantify number of
155 staining-positive cells: 0 = below the limit of detection; 1 = <1%; 2 = 1-33%; 3 = 34-66%; and 4
156 = >66% of cells. For these anatomic regions (e.g. airway or alveoli), cell counts for each tissue
157 were made to know the population density per microscopic field to make reproducible
158 interpretations. For determination of AT2 cell size, ACE2 and SP-C protein immunostaining
159 were evaluated on the same lung tissue section for each case. A region of minimally diseased
160 lung was examined and SP-C⁺ AT2 cells were measured for diameter in the plane perpendicular
161 to the basement membrane. Similar measurements were then made for ACE2⁺/SP-C⁺ cells.

162

163 **Analysis of single cell RNA sequencing data:**

164 Single cell RNA sequencing data sets were accessed from Gene Expression Omnibus (GEO)
165 series GSE121600 (27) and GSE122960 (26). We included samples in our analysis if over 75%
166 cell barcodes had >3000 unique molecular identifiers (UMI) in order to allow accurate cell type
167 calls and clustering. Within samples passing our inclusion criteria, we retained cell barcodes with
168 >1000 UMI. For GSE121600, raw H5 files for bronchial biopsy (GSM3439925), nasal brushing
169 (GSM3439926), and turbinate (GSM3439927) samples were downloaded. Within series
170 GSE121600, sample GSM3439925 (bronchial biopsy), 82% cell barcodes had less than 3000
171 UMI, so the sample was excluded from analysis. The turbinate sample was a biopsy from a 30-
172 year-old female and the nasal brushing was performed in the inferior turbinate of a 56-year-old
173 healthy male donor. For GSE122960, filtered H5 files for eight lung transplant donor samples
174 from lung parenchyma (GSM3489182, GSM3489185, GSM3489187, GSM3489189,
175 GSM3489191, GSM3489193, GSM3489195, GSM3489197) were downloaded. The eight
176 donors varied from 21-63 years of age (median age = 48) and were composed of five African
177 American, one Asian, and two white donors, and 2 active, 1 former, and 5 never smokers. Gene
178 count matrices from the eight donors were aggregated for analysis.

179
180 Gene-by-barcode count matrices were normalized, log-transformed, and scaled followed by
181 dimension reduction using principal components analysis (PCA). Principal components were
182 used to obtain uniform manifold approximation and projection (UMAP) visualizations, and cells
183 were clustered using a shared nearest neighbor (SNN) approach with resolution parameter 0.4,
184 giving 14 clusters for nasal brushing, 15 clusters for turbinate, and 28 clusters for lung
185 parenchyma. Cell types associated with each cluster were identified by determining marker

186 genes for each cluster and comparing the list of marker genes to known cell type markers
187 ([Supplemental Figure 5](#)). All analyses were performed using R package Seurat version 3.1.1
188 (34). In the nasal brushing sample, we were unable to associate a cell type with one cluster
189 containing 776 cells (16.5%) due to low UMIs, so these cells were discarded.

190

191 For the lung parenchyma data, gene expression in alveolar type II cells for a single donor was
192 quantified by summing up gene counts for all alveolar type II cells and dividing by total UMIs
193 for all alveolar type II cells to get normalized counts, followed by rescaling the normalized
194 counts to obtain counts per million (CPM).

195

196 **Statistical analyses:**

197 Statistical analyses for group comparisons and tissue scoring data were performed using
198 GraphPad Prism version 8 (GraphPad Software, La Jolla, CA USA). Mann Whitney U tests or T-
199 tests were used for group comparisons as appropriate. ACE2 protein detection in different tissues
200 was analyzed using the ordinal scoring system (0-4) and Cochran-Armitage test for trend.

201

202 **Role of funding source:**

203 The funding sources had no role in the study design, data collection, data analysis, interpretation,
204 writing, nor decision to publish. The authors have not been paid to write this article by any
205 agency.

206 **Results:**

207 In the alveoli, ACE2 transcripts were detected mostly in alveolar type II (AT2) cells (89·5% of
208 all ACE2⁺ cells) (Figure 1a), but specifically within a subset of these cells (1·2% of AT2 cells)
209 (Figure 1b, Supplemental Figure 1a-b). These data indicate ACE2 transcripts are uncommon in
210 most alveolar cell types. Alveoli had apical ACE2 protein only in a small number (usually ~1%
211 or less) of AT2 cells (Figure 1c), consistent with the scRNA-seq results. The identity of these
212 cells was confirmed by co-staining for surfactant protein-C. These ACE2⁺ AT2 cells were
213 observed within areas of alveolar collapse (Figures 1d-f) and had morphologic features of
214 hyperplastic AT2 cells, being more plump and larger than ACE2⁻ AT2 cells in the same tissue
215 section (Figure 1g). Interestingly, alveolar macrophages were negative for ACE2 protein staining
216 by immunohistochemistry, despite previous reports of ACE2 protein in these cells (Supplemental
217 Table 1). The lack of ACE2 transcripts in macrophages was also confirmed by scRNA-seq data
218 that revealed ACE2 mRNA in only 0·1% of macrophages, monocytes, or dendritic cells
219 (Supplemental Figure 1a-b). The concordance between scRNA-seq and immunohistochemistry
220 results provides compelling evidence that ACE2 is primarily present in a subset of AT2 cells and
221 that alveolar macrophages lack ACE2.

222

223 Recent evidence indicates that proteases such as TMPRSS2 facilitate entry of SARS-CoV-2 into
224 ACE2⁺ cells (35). We evaluated scRNA-seq data and observed that TMPRSS2 mRNA was
225 present in 35·5% of all AT2 cells (Figure 2a) but was more prevalent (50·0%) in ACE2⁺ AT2
226 cells (Figure 2b). Additionally, we observed colocalization of ACE2 and TMPRSS2 on the apical
227 membrane of these AT2 cells (Figure 2c). These findings suggest that AT2 cells with apical

228 ACE2 and TMPRSS2 could readily facilitate SARS-CoV-2 cellular infection and disease as seen
229 in COVID-19 patients.

230

231 We next evaluated ACE2 in the conducting airways (trachea, bronchi, bronchioles). In the
232 trachea and bronchi, apical ACE2 was rare and limited to ciliated cells ([Figure 3a](#)), similar to
233 localization results in primary cultures of well-differentiated human airway epithelial cells (30).
234 In the submucosal glands of large airways, occasional serous cells and vessels near the acini
235 were positive for ACE2 ([Supplemental Figures 2a-b](#)). In bronchioles, ACE2 was regionally
236 localized ([Figures 3b-d](#)). These findings show nominal detection of ACE2, corresponding with
237 the lack of primary airway disease (e.g., bronchitis, etc.) seen in COVID-19 patients.

238

239 Detection of ACE2 protein has been variably reported in several small studies (21, 23). In this
240 larger study, we saw that the regional distribution of ACE2 protein varied between donors. In the
241 surface epithelium of trachea and bronchi, we detected ACE2 in only 12% and 27% of donors,
242 respectively ([Figure 4a](#)). In the distal areas of the lung, ACE2 detection was more common, with
243 bronchiolar and alveolar protein detection in 36% and 59% of donors, respectively ([Figure 4a](#)). A
244 similar pattern of variable alveolar ACE2 was seen for mRNA transcripts in the scRNA-seq data,
245 where 50% of donors showed lower abundance in AT2 cells, and the other 50% of donors showed
246 higher abundance in the same cell type ([Figure 4b](#)). These findings suggest that ACE2
247 expression can vary between different lung regions and between individuals. Importantly, this
248 low level of cellular protein provided us with an opportunity to investigate the potential for
249 various clinical factors to increase ACE2 expression.

250

251 Independent risk factors associated with severe COVID-19 include male sex, increased age, and
252 presence of comorbidities (6, 8-10, 36-38). To evaluate whether the spatial distribution and
253 abundance of ACE2 protein in the lower respiratory tract differed by these risk factors, we
254 scored tissues for ACE2 protein detection ([Supplemental Table 2](#)). In the cohort, neither age nor
255 sex were associated with ACE2 protein detection (using the median age as cut-off) ([Figures 4c-](#)
256 [d](#)). Since recent studies of COVID-19 infections suggested that young children have reduced
257 disease severity when infected by SARS-CoV-2 (6, 7), we compared lung tissue samples from
258 children <10 years of age to those from the remaining older subjects (19-71 years of age) and
259 found that ACE2 protein detection was higher in this subset of young children ([Figure 4e](#)). To
260 test whether ACE2 distribution was affected by the presence of underlying diseases, we assessed
261 the ACE2 localization pattern using tissues from subjects with chronic comorbidities (asthma,
262 cardiovascular disease, chronic obstructive pulmonary disease, cystic fibrosis, diabetes, and
263 smoking) and compared them to controls ([Supplemental Table 2](#)). The control group was similar
264 in age to the chronic disease group ([Figure 4f](#)). We observed no significant differences between
265 the two groups in ACE2 distribution, except for bronchioles, where ACE2 protein was reduced
266 in the chronic disease group ([Figure 4g, Supplemental Figure 2c](#)). These results show that ACE2
267 levels in the respiratory tract were not increased in association with risk factors for severe
268 COVID-19, such as male sex, advanced age, and underlying chronic comorbidities. Instead, we
269 saw increased ACE2 detection in children <10 years of age and in the small airways
270 (bronchioles) of individuals without chronic comorbidities in our cohort, both groups with a
271 lower risk for severe clinical disease.

272

273 Given the unexpected heterogeneity in the lower respiratory tract, we also investigated ACE2 in
274 the upper respiratory tract. scRNA-seq data from nasal brushing and nasal turbinate samples (27)
275 show ACE2 mRNA transcripts in 2-6% of epithelial cells ([Supplemental Figure 3a-d](#)). We then
276 studied nasal biopsy tissues and found that ACE2 protein was detected in all tissue samples and,
277 when present, was seen exclusively on the apical surface of ciliated cells. Distribution varied
278 regionally based on the characteristics of the epithelium, with rare detection in thicker ciliated
279 pseudostratified epithelium, and more abundant protein in thinner epithelium ([Figures 5a-g](#)).
280 Thinner epithelial height is expected in specific regions including the floor of the nasal cavity,
281 meatuses, and paranasal sinuses (39). The sinonasal cavity is an interface between the respiratory
282 tract and the environment, and high SARS-CoV-2 viral loads can be detected in nasal swabs
283 from infected patients (40), consistent with our ACE2 expression data. This reservoir of ACE2⁺
284 cells may facilitate the reported transmission from individuals who have very mild or
285 asymptomatic disease (41).

286 **Discussion:**

287 A critical aspect of this study was to evaluate ACE2 protein expression and distribution by
288 immunohistochemistry to more accurately corroborate single cell transcript studies and better
289 evaluate clinical groups for COVID-19 disease susceptibility. Previously, limited reports have
290 variably shown ACE2 protein in the upper and lower respiratory tract, but cellular localization
291 and distribution in human lung tissues have been inconsistent and contradictory (20-23)
292 ([Supplemental Table 1](#)). *In vitro* studies demonstrate that ACE2 protein is found at the apical
293 membrane of polarized airway epithelia, where it permits virus binding and cell entry (21, 30). In
294 our study, ACE2 was consistently localized to the apical membranes of cells. ACE2 was more
295 commonly found in the sinonasal cavity where transmission likely occurs and on AT2 cells of
296 the lung parenchyma where severe disease develops. We speculate that expression of ACE2 in
297 regions of the sinonasal cavity could explain the high transmissibility of SARS-CoV, SARS-
298 CoV-2, and HCoV-NL63, a cold-related coronavirus which also uses ACE2 as a receptor.
299
300 SARS-CoV and SARS-CoV-2 both replicate in the lungs (42, 43), consistent with the ACE2
301 protein distribution defined in this study and suggested by previous studies (20, 21). We show
302 that ACE2 and TMPRSS2 coexpress in AT2 cells at the mRNA and protein levels, suggesting
303 susceptibility to infection. Additionally, it may also be possible that TMPRSS2⁻ ACE2⁺ AT2
304 cells can become infected through the use of other airway proteases (44). AT2 cells are critical
305 for surfactant protein production and serve as progenitor cells for the AT1 cells, thus damage to
306 these AT2 cells could contribute to acute lung injury (45), which is a common feature of severe
307 COVID-19 (5). Additionally, the larger morphology of ACE2⁺ AT2 cells is consistent with a
308 type of hyperplastic AT2 population that, if damaged, could affect the repair mechanisms of the

309 alveoli. Infection of AT2 cells could disrupt epithelial integrity leading to alveolar edema, and
310 facilitate viral spread to ACE2⁺ interstitial cells/vessels for systemic virus dissemination, given
311 that SARS-CoV-2 has been detected in pulmonary endothelium (46) and blood (47).
312 Furthermore, cell-to-cell spread of coronaviruses to other epithelial cells after initial infection
313 could also occur via receptor-independent mechanisms related to the fusogenic properties of the
314 S protein (48). It is interesting that computerized tomography studies of early disease in people
315 with COVID-19 demonstrate patchy ground glass opacities in the peripheral and posterior lungs,
316 regions that are more susceptible to alveolar collapse (49).
317
318 ACE2 protein detection in the lower respiratory tract was heterogeneous. The relatively small
319 number of ACE2⁺ cells found in our study proved advantageous in evaluating whether
320 conditions that predispose to severe disease also increased cellular ACE2 expression, but this
321 was not observed. Rather we saw elevated ACE2 protein in demographic pools with expected
322 low risk for severe COVID-19 (young children and in bronchioles of the control group) and
323 these results suggest alternative explanations. First, the potential relationship between ACE2
324 abundance in the respiratory tract and severe COVID-19 is likely complex. On one hand, more
325 receptor availability could enhance viral entry into cells and worsen disease outcomes;
326 alternatively, ACE2 may play a protective role in acute lung injury through its enzymatic activity
327 (50-52) and therefore could improve disease outcomes. Our data would support the latter and
328 implicate a dualistic role for ACE2 as both a viral receptor and a protective agent in acute lung
329 injury. Additionally, ACE2 exists in cell-associated and soluble forms (53). It is possible that
330 greater ACE2 expression could result in increased soluble ACE2 in respiratory secretions where
331 it might act as a decoy receptor and reduce virus entry (1, 54). Second, other factors such as

332 TMPRSS2 expression might be more important in regulating disease severity. TMPRSS2 on the
333 apical membrane of AT2 cells might facilitate SARS-CoV-2 entry when ACE2 is rare or even
334 below the limit of detection in this study. Third, low levels of the receptor could be sufficient for
335 the virus to infect and cause severe disease. Importantly, unlike SARS or HCoV-NL63, the
336 SARS-CoV-2 spike glycoproteins undergo proteolytic processing at a multibasic S1/S2 site by
337 furin intracellularly, prior to virion release (35, 55). Additionally, compared to SARS-CoV, the
338 SARS-CoV-2 receptor binding motif has a higher affinity for ACE2 (56, 57). These features may
339 enhance the ability of SARS-CoV-2 to bind to cells, undergo S2' cleavage by TMPRSS2 or other
340 surface proteases, fuse to the host cell membrane, and release its genome. Finally, we
341 acknowledge that it is possible that SARS-CoV-2 infection could modify ACE2 expression in
342 the respiratory tract, or that ACE2 expression in other organs could impact disease severity. It is
343 important to mention that the lack of correlation between SARS-CoV-2 receptor expression and
344 disease severity contrasts with another severe coronavirus disease, MERS, where comorbidities
345 were observed to increase its receptor detection in respiratory tissues (58, 59).

346
347 mRNA transcript abundance is not always representative of protein levels (60), and therefore
348 both should be evaluated in conjunction before making conclusions about gene expression. Some
349 of the factors that account for these differences include post-transcriptional regulation or rapid
350 protein turnover. Additionally, other factors limit direct comparisons between scRNA-seq results
351 and protein staining, including sample size, tissue heterogeneity, and undefined biopsy sites. In
352 the alveoli, we show ACE2 protein in a small subset of AT2 cells, which correlates with the
353 scRNA-seq data and with other RNA sequencing publications (14, 18, 19). In the lower airways
354 and sinonasal cavity, RNA sequencing data indicate ACE2 transcripts in both ciliated and

355 secretory cells (14, 18, 19), but we show ACE2 protein is only found in ciliated cells. Likewise,
356 some authors have reported lower ACE2 transcript abundance in children (12, 15) and suggested
357 this finding as an explanation for the lower disease severity in this age group. In contrast, we
358 show that children do not have less ACE2 protein than older adults, and while children appear
359 protected from severe lung disease, they are likely at similar risk for infection (7, 61, 62).

360

361 In summary, we find that ACE2 protein has heterogeneous expression in the respiratory tract
362 with more frequent ACE2 detection in the sinonasal epithelium and AT2 cells that correlates
363 with putative sites for transmission and severe disease, respectively. The small subset of ACE2⁺
364 AT2 cells in the lung could be further studied to reveal factors regulating ACE2 expression and
365 clarify potential targets for antiviral therapies. Contrary to our initial hypothesis, we saw no
366 increase of ACE2 protein in the chronic disease group. Interestingly, we observed increased
367 ACE2 in young children and control group bronchioles, suggesting a possible protective effect
368 by ACE2 expression. These results suggest that features driving disease susceptibility and
369 severity are complex. Factors other than ACE2 protein abundance, including viral load, host
370 innate and adaptive immune responses, and the activities of the pulmonary renin-angiotensin
371 system may also be important determinants of outcomes.

372 **Author contributions:**

373 Conceptualization and writing – original draft, M. E.O.B., P.B.M. and D.K.M.; Data curation,
374 A.T.; Formal analysis, M. E.O.B., A.T., A. A.P. and D.K.M.; Investigation, A.T., A. A.P.,
375 M.R.L., C.W.-L. and D.K.M.; Visualization, M. E.O.B., A.T., D.K.M.; Resources, A. A.P.,
376 J.A.K.-T., P.H.K., P.T., P.B.M. and D.K.M.; Writing – review and editing, M. E.O.B, A.T., A.
377 A.P., M.R.L., J.A.K.-T., P.H.K., P.T., C.W.-L., P.B.M. and D.K.M.
378 All authors approved the final version of this manuscript.

379 **Funding sources:**

380 This work is supported by the National Institutes of Health (NIH) Grant P01 AI060699; and the
381 Pathology Core, which are partially supported by the Center for Gene Therapy for Cystic
382 Fibrosis (NIH Grant P30 DK-54759), and the Cystic Fibrosis Foundation. P.B.M. is supported by
383 the Roy J. Carver Charitable Trust.

384 **Declaration of interests:**

385 The authors declare no competing interests related to this work. This work was supported by the
386 National Institutes of Health (NIH, P01 AI060699). P.B.M. is on the scientific advisory board
387 and receives support for sponsored research from Spirovant Sciences, Inc. P.B.M. is on the
388 scientific advisory board for Oryn Therapeutics.

389 **Acknowledgements:**

390 We thank our laboratory members and colleagues Stanley Perlman, Robert Robinson, and Tom
391 Gallagher for their helpful discussion and technical assistance.

392 **Data sharing statement:**

393 All single-cell RNA sequencing datasets used in this manuscript are publicly available as
394 outlined in the Methods.

395 **References:**

- 396 1. Li W, Moore MJ, Vasilieva N, Sui J, Wong SK, Berne MA, et al. Angiotensin-converting enzyme
397 2 is a functional receptor for the SARS coronavirus. *Nature*. 2003;426(6965):450-4.
- 398 2. Zhou P, Yang XL, Wang XG, Hu B, Zhang L, Zhang W, et al. A pneumonia outbreak associated
399 with a new coronavirus of probable bat origin. *Nature*. 2020.
- 400 3. Lam CW, Chan MH, Wong CK. Severe acute respiratory syndrome: clinical and laboratory
401 manifestations. *Clin Biochem Rev*. 2004;25(2):121-32.
- 402 4. Wilder-Smith A, Chiew CJ, Lee VJ. Can we contain the COVID-19 outbreak with the same
403 measures as for SARS? *Lancet Infect Dis*. 2020.
- 404 5. Zhou F, Yu T, Du R, Fan G, Liu Y, Liu Z, et al. Clinical course and risk factors for mortality of
405 adult inpatients with COVID-19 in Wuhan, China: a retrospective cohort study. *Lancet*. 2020.
- 406 6. Guan WJ, Ni ZY, Hu Y, Liang WH, Ou CQ, He JX, et al. Clinical Characteristics of Coronavirus
407 Disease 2019 in China. *N Engl J Med*. 2020.
- 408 7. Dong Y, Mo X, Hu Y, Qi X, Jiang F, Jiang Z, et al. Epidemiology of COVID-19 Among
409 Children in China. *Pediatrics*. 2020.
- 410 8. Liu W, Tao ZW, Wang L, Yuan ML, Liu K, Zhou L, et al. Analysis of factors associated with
411 disease outcomes in hospitalized patients with 2019 novel coronavirus disease. *Chin Med J (Engl)*.
412 2020;133(9):1032-8.
- 413 9. Wu J, Zhang J, Sun X, Wang L, Xu Y, Zhang Y, et al. Influence of diabetes mellitus on the
414 severity and fatality of SARS-CoV-2 (COVID-19) infection. *Diabetes Obes Metab*. 2020.
- 415 10. Yang J, Zheng Y, Gou X, Pu K, Chen Z, Guo Q, et al. Prevalence of comorbidities and its effects
416 in patients infected with SARS-CoV-2: a systematic review and meta-analysis. *Int J Infect Dis*.
417 2020;94:91-5.
- 418 11. Wu Y, Guo W, Liu H, Qi B, Liang K, Xu H, et al. Clinical outcomes of 402 patients with
419 COVID-2019 from a single center in Wuhan, China. *J Med Virol*. 2020.
- 420 12. Bunyavanich S, Do A, Vicencio A. Nasal Gene Expression of Angiotensin-Converting Enzyme 2
421 in Children and Adults. *JAMA*. 2020.
- 422 13. Li G, He X, Zhang L, Ran Q, Wang J, Xiong A, et al. Assessing ACE2 expression patterns in
423 lung tissues in the pathogenesis of COVID-19. *J Autoimmun*. 2020:102463.
- 424 14. Lukassen S, Chua RL, Trefzer T, Kahn NC, Schneider MA, Muley T, et al. SARS-CoV-2
425 receptor ACE2 and TMPRSS2 are primarily expressed in bronchial transient secretory cells. *EMBO J*.
426 2020;39(10):e105114.
- 427 15. Muus C, Luecken MD, Eraslan G, Waghray A, Heimberg G, Sikkema L, et al. Integrated
428 analyses of single-cell atlases reveal age, gender, and smoking status associations with cell type-specific
429 expression of mediators of SARS-CoV-2 viral entry and highlights inflammatory programs in putative
430 target cells. *bioRxiv*. 2020.
- 431 16. Pinto BG, Oliveira AE, Singh Y, Jimenez L, Goncalves AN, Ogava RL, et al. ACE2 Expression
432 is Increased in the Lungs of Patients with Comorbidities Associated with Severe COVID-19. *medRxiv*.
433 2020.
- 434 17. Smith JC, Sausville EL, Girish V, Yuan ML, Vasudevan A, John KM, et al. Cigarette smoke
435 exposure and inflammatory signaling increase the expression of the SARS-CoV-2 receptor ACE2 in the
436 respiratory tract. *Dev Cell*. 2020.
- 437 18. Sungnak W, Huang N, Becavin C, Berg M, Queen R, Litvinukova M, et al. SARS-CoV-2 entry
438 factors are highly expressed in nasal epithelial cells together with innate immune genes. *Nat Med*.
439 2020;26(5):681-7.
- 440 19. Ziegler CGK, Allon SJ, Nyquist SK, Mbanjo IM, Miao VN, Tzouanas CN, et al. SARS-CoV-2
441 Receptor ACE2 Is an Interferon-Stimulated Gene in Human Airway Epithelial Cells and Is Detected in
442 Specific Cell Subsets across Tissues. *Cell*. 2020.

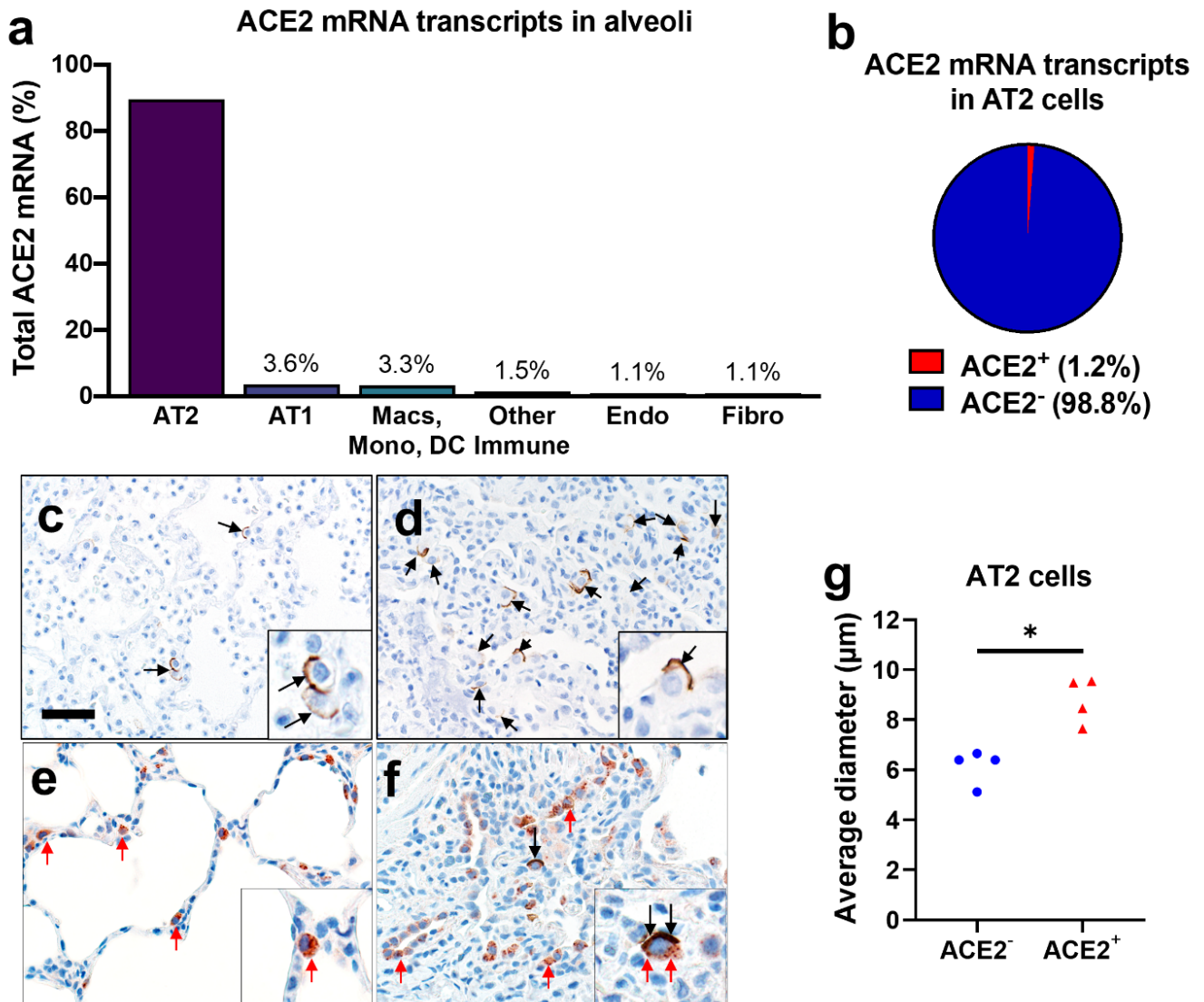
- 443 20. Hamming I, Timens W, Bulthuis ML, Lely AT, Navis G, van Goor H. Tissue distribution of
444 ACE2 protein, the functional receptor for SARS coronavirus. A first step in understanding SARS
445 pathogenesis. *J Pathol.* 2004;203(2):631-7.
- 446 21. Ren X, Glende J, Al-Falah M, de Vries V, Schwegmann-Wessels C, Qu X, et al. Analysis of
447 ACE2 in polarized epithelial cells: surface expression and function as receptor for severe acute respiratory
448 syndrome-associated coronavirus. *J Gen Virol.* 2006;87(Pt 6):1691-5.
- 449 22. Bertram S, Glowacka I, Muller MA, Lavender H, Gnirss K, Nehlmeier I, et al. Cleavage and
450 activation of the severe acute respiratory syndrome coronavirus spike protein by human airway trypsin-
451 like protease. *J Virol.* 2011;85(24):13363-72.
- 452 23. Bertram S, Heurich A, Lavender H, Gierer S, Danisch S, Perin P, et al. Influenza and SARS-
453 coronavirus activating proteases TMPRSS2 and HAT are expressed at multiple sites in human respiratory
454 and gastrointestinal tracts. *PLoS One.* 2012;7(4):e35876.
- 455 24. Carrel L, Willard HF. X-inactivation profile reveals extensive variability in X-linked gene
456 expression in females. *Nature.* 2005;434(7031):400-4.
- 457 25. Anguiano L, Riera M, Pascual J, Soler MJ. Circulating ACE2 in Cardiovascular and Kidney
458 Diseases. *Curr Med Chem.* 2017;24(30):3231-41.
- 459 26. Reyfman PA, Walter JM, Joshi N, Anekalla KR, McQuattie-Pimentel AC, Chiu S, et al. Single-
460 Cell Transcriptomic Analysis of Human Lung Provides Insights into the Pathobiology of Pulmonary
461 Fibrosis. *Am J Respir Crit Care Med.* 2019;199(12):1517-36.
- 462 27. Ruiz Garcia S, Deprez M, Lebrigand K, Cavard A, Paquet A, Arguel MJ, et al. Novel dynamics
463 of human mucociliary differentiation revealed by single-cell RNA sequencing of nasal epithelial cultures.
464 *Development.* 2019;146(20).
- 465 28. Itani OA, Chen JH, Karp PH, Ernst S, Keshavjee S, Parekh K, et al. Human cystic fibrosis airway
466 epithelia have reduced Cl⁻ conductance but not increased Na⁺ conductance. *Proc Natl Acad Sci U S A.*
467 2011;108(25):10260-5.
- 468 29. Meyerholz DK, Suarez CJ, Dintzis SM, Frevert CW. *Comparative Anatomy and Histology: A*
469 *Mouse, Rat and Human Atlas.* 2nd ed: Academic Press - Elsevier; 2018.
- 470 30. Jia HP, Look DC, Shi L, Hickey M, Pewe L, Netland J, et al. ACE2 receptor expression and
471 severe acute respiratory syndrome coronavirus infection depend on differentiation of human airway
472 epithelia. *J Virol.* 2005;79(23):14614-21.
- 473 31. Krishnamurthy S, Wohlford-Lenane C, Kandimalla S, Sartre G, Meyerholz DK, Theberge V, et
474 al. Engineered amphiphilic peptides enable delivery of proteins and CRISPR-associated nucleases to
475 airway epithelia. *Nat Commun.* 2019;10(1):4906.
- 476 32. Meyerholz DK, Lambert AM, Reznikov LR, Ofori-Amanfo GK, Karp PH, McCray PB, Jr., et al.
477 Immunohistochemical Detection of Markers for Translational Studies of Lung Disease in Pigs and
478 Humans. *Toxicol Pathol.* 2016;44(3):434-41.
- 479 33. Meyerholz DK, Beck AP. Principles and approaches for reproducible scoring of tissue stains in
480 research. *Lab Invest.* 2018;98(7):844-55.
- 481 34. Stuart T, Butler A, Hoffman P, Hafemeister C, Papalexi E, Mauck WM, 3rd, et al.
482 Comprehensive Integration of Single-Cell Data. *Cell.* 2019;177(7):1888-902 e21.
- 483 35. Hoffmann M, Kleine-Weber H, Schroeder S, Kruger N, Herrler T, Erichsen S, et al. SARS-CoV-
484 2 Cell Entry Depends on ACE2 and TMPRSS2 and Is Blocked by a Clinically Proven Protease Inhibitor.
485 *Cell.* 2020.
- 486 36. Lu Q, Shi Y. Coronavirus disease (COVID-19) and neonate: What neonatologist need to know. *J*
487 *Med Virol.* 2020.
- 488 37. Mo P, Xing Y, Xiao Y, Deng L, Zhao Q, Wang H, et al. Clinical characteristics of refractory
489 COVID-19 pneumonia in Wuhan, China. *Clin Infect Dis.* 2020.
- 490 38. Tian S, Liu H, Liao M, Wu Y, Yang C, Cai Y, et al. Analysis of Mortality in Patients With
491 COVID-19: Clinical and Laboratory Parameters. *Open Forum Infect Dis.* 2020;7(5):ofaa152.

- 492 39. Sternberg SS. *Histology for Pathologists*. 2nd ed. Philadelphia, PA USA: Lippincott-Raven
493 Publishers; 1997.
- 494 40. Wang W, Xu Y, Gao R, Lu R, Han K, Wu G, et al. Detection of SARS-CoV-2 in Different Types
495 of Clinical Specimens. *JAMA*. 2020.
- 496 41. Bai Y, Yao L, Wei T, Tian F, Jin DY, Chen L, et al. Presumed Asymptomatic Carrier
497 Transmission of COVID-19. *JAMA*. 2020.
- 498 42. Yen YT, Liao F, Hsiao CH, Kao CL, Chen YC, Wu-Hsieh BA. Modeling the early events of
499 severe acute respiratory syndrome coronavirus infection in vitro. *J Virol*. 2006;80(6):2684-93.
- 500 43. Zhang H, Zhou P, Wei Y, Yue H, Wang Y, Hu M, et al. Histopathologic Changes and SARS-
501 CoV-2 Immunostaining in the Lung of a Patient With COVID-19. *Ann Intern Med*. 2020.
- 502 44. Ou X, Liu Y, Lei X, Li P, Mi D, Ren L, et al. Characterization of spike glycoprotein of SARS-
503 CoV-2 on virus entry and its immune cross-reactivity with SARS-CoV. *Nat Commun*. 2020;11(1):1620.
- 504 45. Ware LB, Matthay MA. The acute respiratory distress syndrome. *N Engl J Med*.
505 2000;342(18):1334-49.
- 506 46. Ackermann M, Verleden SE, Kuehnel M, Haverich A, Welte T, Laenger F, et al. Pulmonary
507 Vascular Endothelialitis, Thrombosis, and Angiogenesis in Covid-19. *N Engl J Med*. 2020.
- 508 47. Chen W, Lan Y, Yuan X, Deng X, Li Y, Cai X, et al. Detectable 2019-nCoV viral RNA in blood
509 is a strong indicator for the further clinical severity. *Emerg Microbes Infect*. 2020;9(1):469-73.
- 510 48. Gallagher TM, Buchmeier MJ, Perlman S. Dissemination of MHV4 (strain JHM) infection does
511 not require specific coronavirus receptors. *Adv Exp Med Biol*. 1993;342:279-84.
- 512 49. Song F, Shi N, Shan F, Zhang Z, Shen J, Lu H, et al. Emerging 2019 Novel Coronavirus (2019-
513 nCoV) Pneumonia. *Radiology*. 2020;295(1):210-7.
- 514 50. Gu H, Xie Z, Li T, Zhang S, Lai C, Zhu P, et al. Angiotensin-converting enzyme 2 inhibits lung
515 injury induced by respiratory syncytial virus. *Sci Rep*. 2016;6:19840.
- 516 51. Imai Y, Kuba K, Rao S, Huan Y, Guo F, Guan B, et al. Angiotensin-converting enzyme 2
517 protects from severe acute lung failure. *Nature*. 2005;436(7047):112-6.
- 518 52. Zou Z, Yan Y, Shu Y, Gao R, Sun Y, Li X, et al. Angiotensin-converting enzyme 2 protects from
519 lethal avian influenza A H5N1 infections. *Nat Commun*. 2014;5:3594.
- 520 53. Lambert DW, Yarski M, Warner FJ, Thornhill P, Parkin ET, Smith AI, et al. Tumor necrosis
521 factor-alpha convertase (ADAM17) mediates regulated ectodomain shedding of the severe-acute
522 respiratory syndrome-coronavirus (SARS-CoV) receptor, angiotensin-converting enzyme-2 (ACE2). *J*
523 *Biol Chem*. 2005;280(34):30113-9.
- 524 54. Hofmann H, Geier M, Marzi A, Krumbiegel M, Peipp M, Fey GH, et al. Susceptibility to SARS
525 coronavirus S protein-driven infection correlates with expression of angiotensin converting enzyme 2 and
526 infection can be blocked by soluble receptor. *Biochem Biophys Res Commun*. 2004;319(4):1216-21.
- 527 55. Hoffmann M, Kleine-Weber H, Pohlmann S. A Multibasic Cleavage Site in the Spike Protein of
528 SARS-CoV-2 Is Essential for Infection of Human Lung Cells. *Mol Cell*. 2020;78(4):779-84 e5.
- 529 56. Shang J, Ye G, Shi K, Wan Y, Luo C, Aihara H, et al. Structural basis of receptor recognition by
530 SARS-CoV-2. *Nature*. 2020;581(7807):221-4.
- 531 57. Wan Y, Shang J, Graham R, Baric RS, Li F. Receptor Recognition by the Novel Coronavirus
532 from Wuhan: an Analysis Based on Decade-Long Structural Studies of SARS Coronavirus. *J Virol*.
533 2020;94(7).
- 534 58. Meyerholz DK, Lambertz AM, McCray PB, Jr. Dipeptidyl Peptidase 4 Distribution in the Human
535 Respiratory Tract: Implications for the Middle East Respiratory Syndrome. *Am J Pathol*. 2016;186(1):78-
536 86.
- 537 59. Seys LJM, Widagdo W, Verhamme FM, Kleinjan A, Janssens W, Joos GF, et al. DPP4, the
538 Middle East Respiratory Syndrome Coronavirus Receptor, is Upregulated in Lungs of Smokers and
539 Chronic Obstructive Pulmonary Disease Patients. *Clin Infect Dis*. 2018;66(1):45-53.
- 540 60. Liu Y, Beyer A, Aebersold R. On the Dependency of Cellular Protein Levels on mRNA
541 Abundance. *Cell*. 2016;165(3):535-50.

- 542 61. Bi Q, Wu Y, Mei S, Ye C, Zou X, Zhang Z, et al. Epidemiology and transmission of COVID-19
543 in 391 cases and 1286 of their close contacts in Shenzhen, China: a retrospective cohort study. *Lancet*
544 *Infect Dis.* 2020.
- 545 62. Sun D, Zhu F, Wang C, Wu J, Liu J, Chen X, et al. Children Infected With SARS-CoV-2 From
546 Family Clusters. *Frontiers in Pediatrics.* 2020;8(386).

547

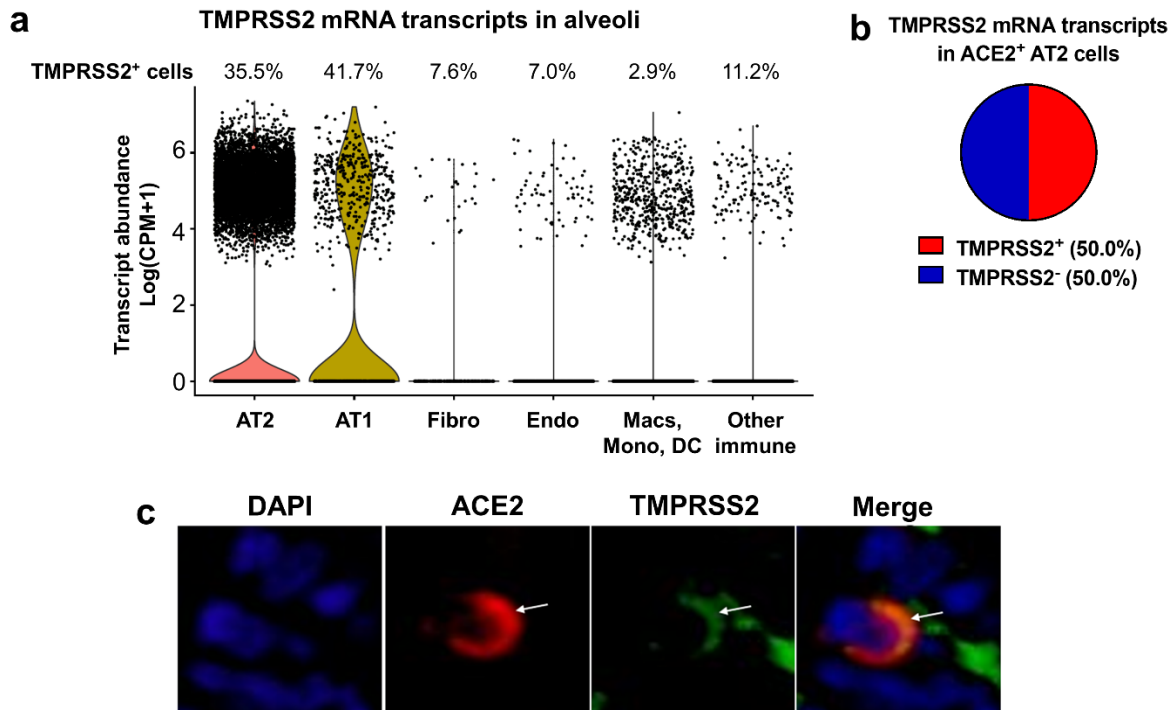
Figure 1



548
549 **Figure 1. ACE2 expression in human lung.** a, b) Single-cell RNA sequencing reanalysis of
550 ACE2 transcript abundance in alveoli from lung parenchyma samples (26). Summative
551 observations from all donors. Airway cells (basal, mitotic, ciliated, club) are not shown. a)
552 89.5% of the cells with detectable ACE2 mRNA in the alveoli are alveolar type II cells. b) Only
553 1.2% of alveolar type II cells have ACE2 mRNA transcripts. c-f) Detection of ACE2 protein
554 (brown color, black arrows, and insets) in representative sections of lower respiratory tract
555 regions and tissue scoring (see Supplemental Table 2) (g). c, d) Alveolar regions had uncommon
556 to regional polarized apical staining of solitary epithelial cells (c) that (when present) were more

557 readily detected in collapsed regions of lung (**d**). **e**, **f**) SP-C (red arrows, inset) and ACE2 (black
558 arrows, inset) dual immunohistochemistry on the same tissue sections. **e**) Non-collapsed regions
559 had normal SP-C⁺ AT2 cells lacking ACE2. **f**) Focal section of peri-airway remodeling and
560 collapse with several SP-C⁺ (red arrows) AT2 cells, but only a small subset of AT2 cells had
561 prominent apical ACE2 protein (black arrows, inset). **g**) SP-C⁺/ACE2⁺ AT2 cells were often
562 larger than SP-C⁺/ACE2⁻ AT2 cells from same lung sections (see also **d** and **e** insets) indicative
563 of AT2 hypertrophy, each data point represents the average value for each case from 5-10 cell
564 measurements per group, P=0.0014, paired T-test. AT2: alveolar type II. AT1: alveolar type I.
565 Macs: Macrophages. Mono: Monocytes. DC: dendritic cells. Other immune cells: B cells, mast
566 cells, natural killer/T cells. Endo: Endothelial. Fibro: Fibroblasts/myofibroblasts. Bar = 35 μ m.

Figure 2

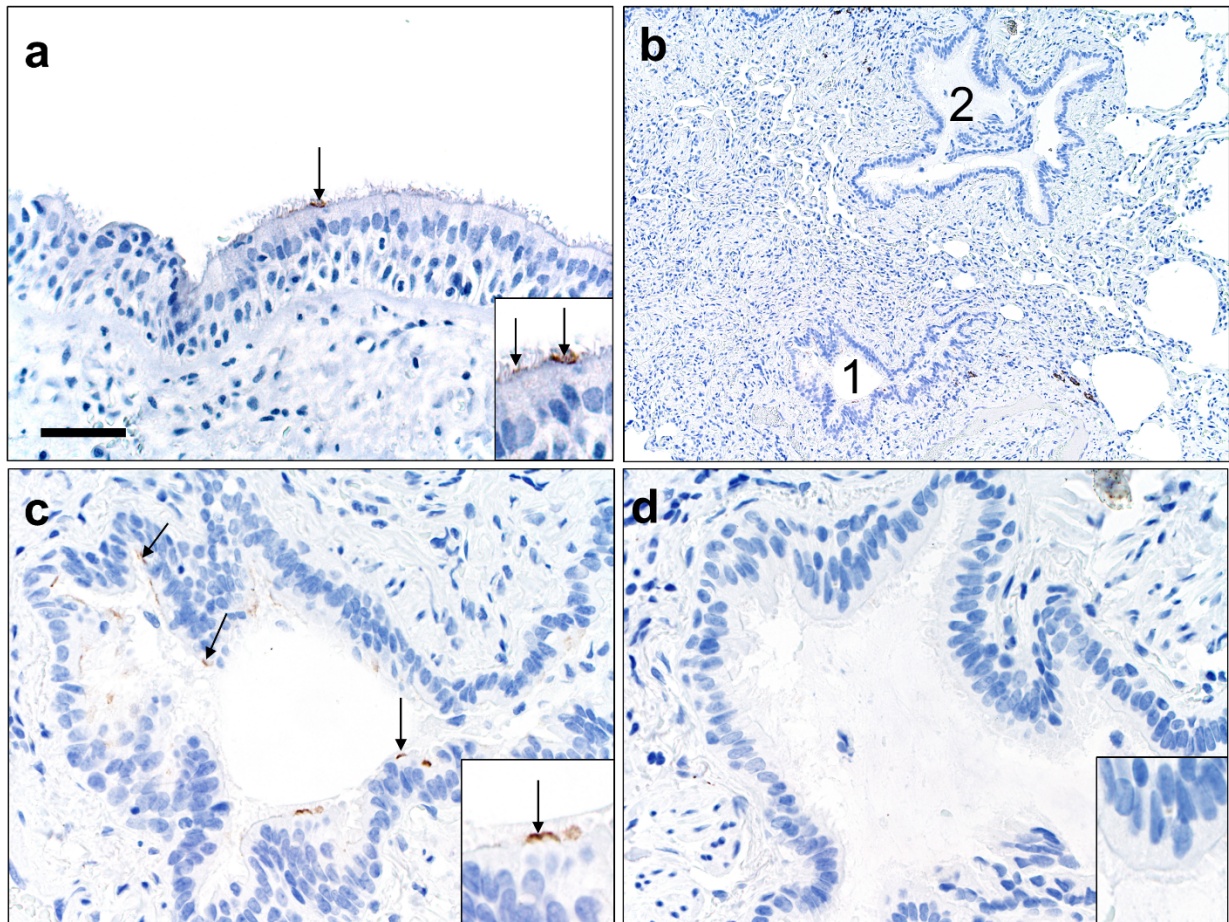


567

568 **Figure 2. TMPRSS2 expression in the alveoli.** **a, b)** Single-cell RNA sequencing reanalyses of
569 TMPRSS2 transcript abundance in alveoli from lung parenchyma (26). Summative observations
570 from all donors. **a)** Percentage of TMPRSS2⁺ cells within each cell type shows TMPRSS2
571 transcripts in 35.5% of alveolar type II cells. Airway cells (basal, mitotic, ciliated, club) are not
572 shown. Violin plots represent expression, each data point denotes a cell. **b)** TMPRSS2 transcripts
573 in ACE2⁺ alveolar type II cells. **c)** Immunofluorescence of alveoli shows apical colocalization of
574 ACE2 and TMPRSS2 (white arrows). AT2: alveolar type II. AT1: alveolar type I. Macs:
575 Macrophages. Mono: Monocytes. DC: dendritic cells. Other immune cells: B cells, mast cells,
576 natural killer/T cells. Endo: Endothelial. Fibro: Fibroblasts/myofibroblasts. CPM: counts per
577 million.

578

Figure 3



579

580 **Figure 3. ACE2 protein in human lower airways. a)** Large airways (trachea and bronchi)

581 exhibited rare ACE2 protein on the apical surface of ciliated cells. **b-d)** Small airways

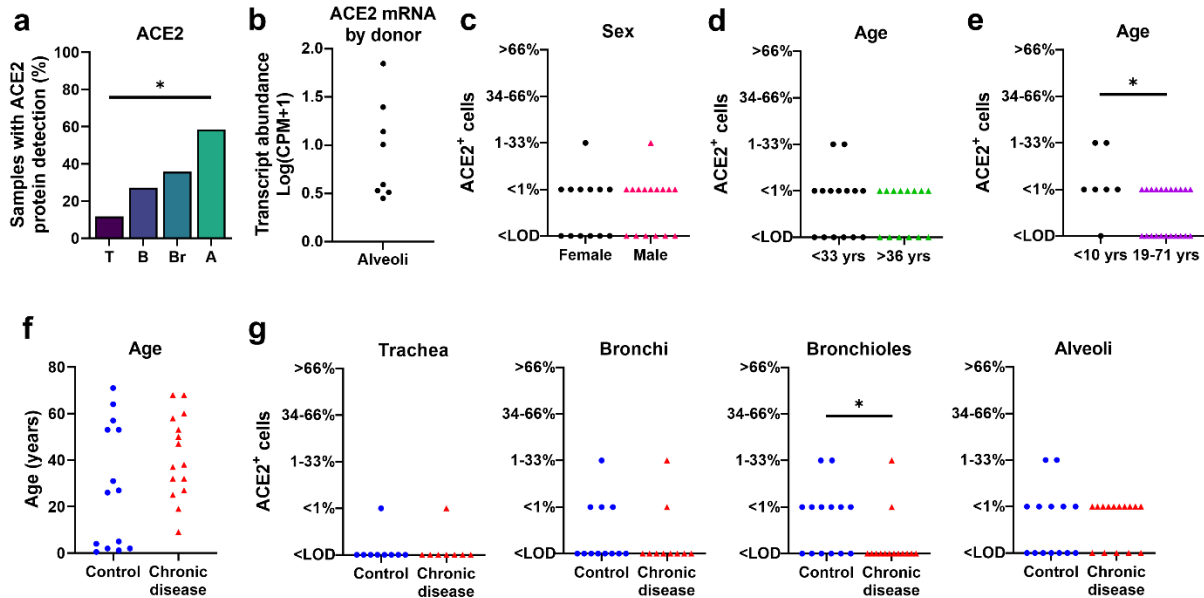
582 (bronchioles) exhibited uncommon to localized apical ACE2 protein in ciliated cells (**c**, #1 in **b**)

583 while the adjacent bronchioles (**d**, #2 in **b**) lacked protein. Bar = 35 (a), 140 (b), and 70 μ m (c,

584 d).

585

Figure 4

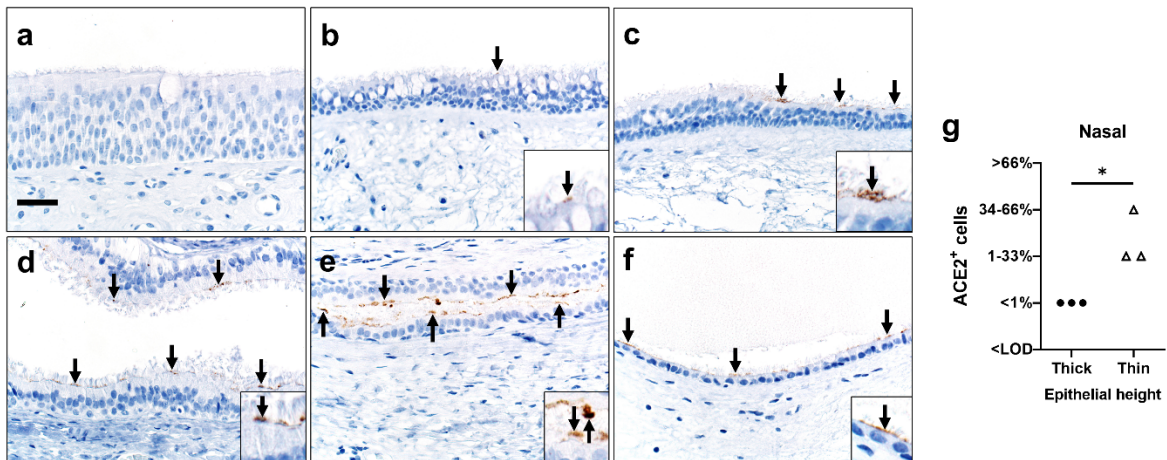


586

587 **Figure 4. ACE2 distribution and scores in respiratory tissues.** **a)** ACE2 protein had
 588 progressively increased detection between donors in tissues from trachea (T), bronchi (B),
 589 bronchioles (Br), to alveoli (A), ($P=0.0009$, Cochran-Armitage test for trend). **b)** Single-cell
 590 RNA sequencing reanalyses of ACE2 mRNA transcript abundance in the alveoli shows variation
 591 between donors (26). **c-d)** ACE2 protein scores from lung donors showed no differences based
 592 on sex or lower vs. upper ages (using median age as a cut-off) (A, $P=0.7338$ and B, $P=0.7053$,
 593 Mann-Whitney U test). **e)** ACE2 protein scores were elevated in young children (<10 yrs)
 594 compared to the remaining subjects (19-71 yrs) ($P=0.0282$ Mann-Whitney U test). **f)** Control and
 595 chronic disease groups did not have any significant differences in age ($P=0.1362$ Mann-Whitney
 596 U test). **g)** ACE2 protein scores for trachea, bronchi, bronchiole, and alveoli in control versus
 597 chronic disease groups ($P= >0.9999$, 0.6263 , 0.0433 , and 0.7359 , respectively, Mann-Whitney
 598 U test). Each symbol represents one donor. CPM: counts per million. LOD: Limit of detection.

599

Figure 5



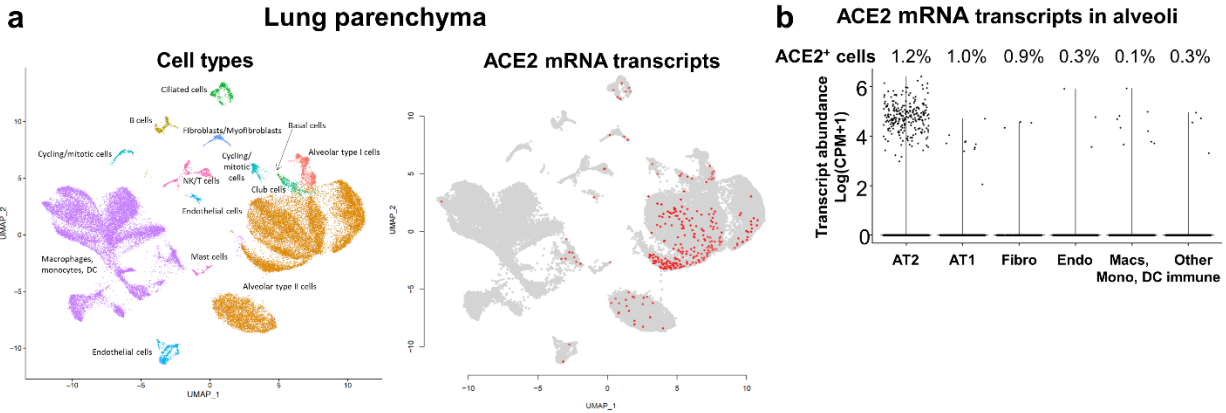
600

601 **Figure 5. ACE2 protein in sinonasal tissues.** Detection of ACE2 protein (brown color, arrows,
602 and insets, **a-f**) and tissue scoring (**g**) in representative sections of nasal tissues. **a, b**) In thick
603 pseudostratified epithelium (PSE) ACE2 protein was absent (**a**) to rare (**b**) and apically located
604 on ciliated cells. **c**) Tissue section shows a transition zone from thick (left side, $> \sim 4$ nuclei) to
605 thin (right side, $\leq \sim 4$ nuclei) PSE and ACE2 protein was restricted to the apical surface of the
606 thin PSE. **d-f**) ACE2 protein was detected multifocally on the apical surface of ciliated cells in
607 varying types of thin PSE, even to simple cuboidal epithelium (**f**). Bar = 30 μm . **g**) ACE2 protein
608 detection scores for each subject were higher in thin than thick epithelium, ($P=0.05$, Mann-
609 Whitney U test). LOD: Limit of detection.

610

611 **Supplemental information:**

Supplemental Figure 1



612

613 **Supplemental Figure 1.** Single-cell RNA sequencing reanalyses of ACE2 transcript abundance

614 in lung parenchyma (26). Summative observations from all donors. **a)** Uniform manifold

615 approximation and projection (UMAP) visualizations. Cells were clustered using a shared

616 nearest neighbor (SNN) approach. Cell types associated with each cluster were identified by

617 determining marker genes for each cluster. Each data point denotes a cell. On the right panel,

618 cells with ACE2 transcripts are shown in red. **b)** Violin plots representing ACE2 expression in

619 the alveoli. Airway cells (basal, mitotic, ciliated, club) are not shown. Percentage of ACE2⁺ cells

620 within each cell type shows ACE2 transcripts in 1.2% of alveolar type II cells and in 0.1% of

621 macrophages, monocytes, or dendritic cells. Each data point denotes a cell, most cells have no

622 expression (0). AT2: alveolar type II. AT1: alveolar type I. Macs: Macrophages. Mono:

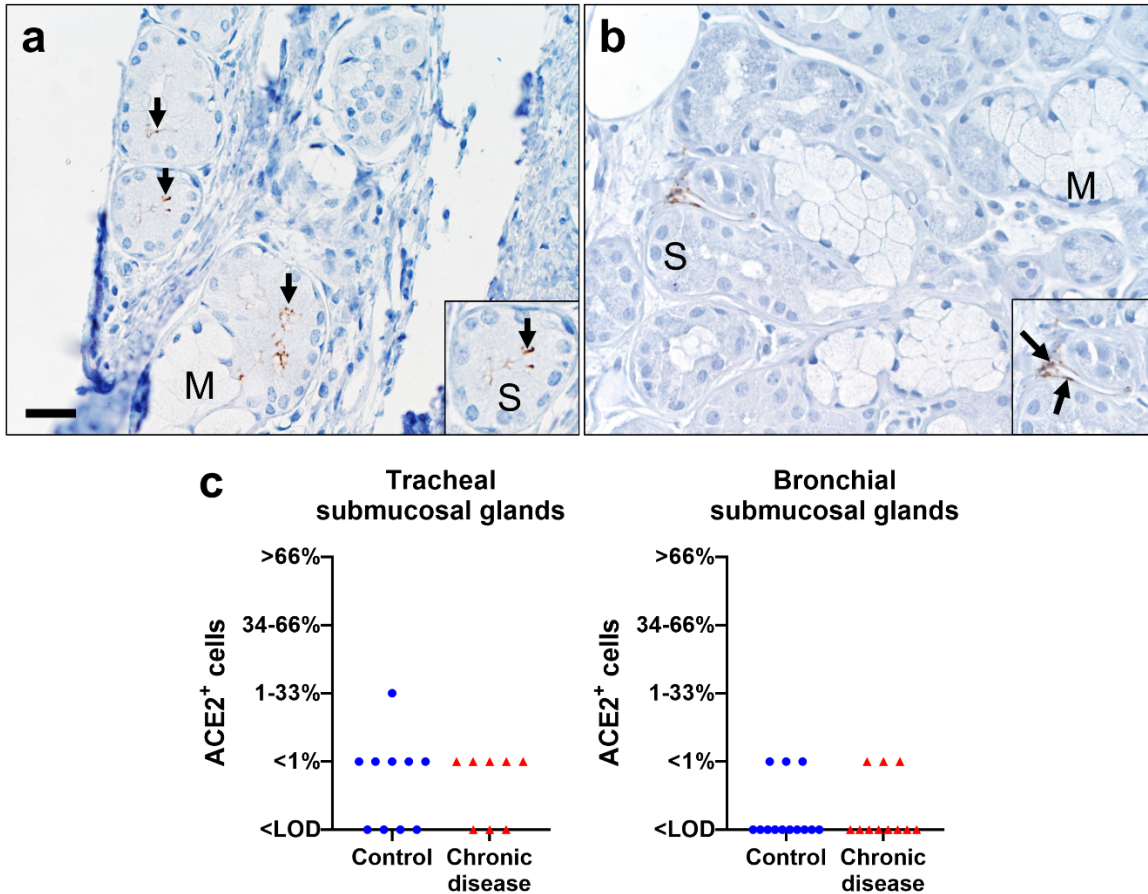
623 Monocytes. DC: dendritic cells. Other immune cells: B cells, mast cells, natural killer/T cells.

624 Endo: Endothelial. Fibro: Fibroblasts/myofibroblasts. NK: Natural killer. CPM: Counts per

625 million.

626

Supplemental Figure 2



627

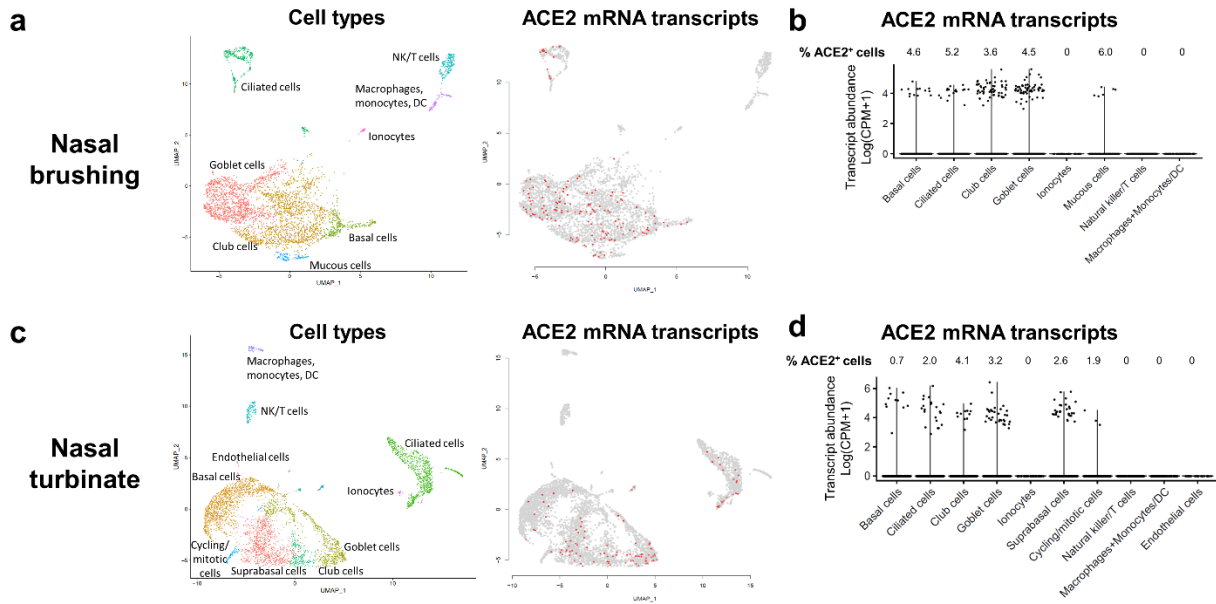
628 **Supplemental Figure 2.** Representative tissue section from submucosa of large airways
629 (trachea/bronchi) showing ACE2 protein localization (brown color, black arrows) (**a**, **b**) and
630 scores (**c**). **a**) Submucosal glands had uncommon to localized apical ACE2 protein (arrows) in
631 serous (S) cells, but not mucous (M) cells. **b**) Submucosal glands also had absent to uncommon
632 ACE2 protein (arrows) in the interstitium that centered on vascular walls and endothelium. This
633 vascular staining was uncommonly seen in lung too and corresponded to the low levels seen in
634 transcripts for these endothelial cells ([Supplemental Figure 1a-b](#)). Note the absence of ACE2
635 staining in serous (S) or mucous (M) cells of the gland (**b**). **c**) ACE2 protein scores for each
636 subject for serous cells in submucosal glands from trachea and bronchi, in control versus chronic

637 disease groups ($P > 0.9999$, 0.9999 , respectively, Mann-Whitney U test). Bar = 25 μm . LOD:

638 Limit of detection.

639

Supplemental Figure 3

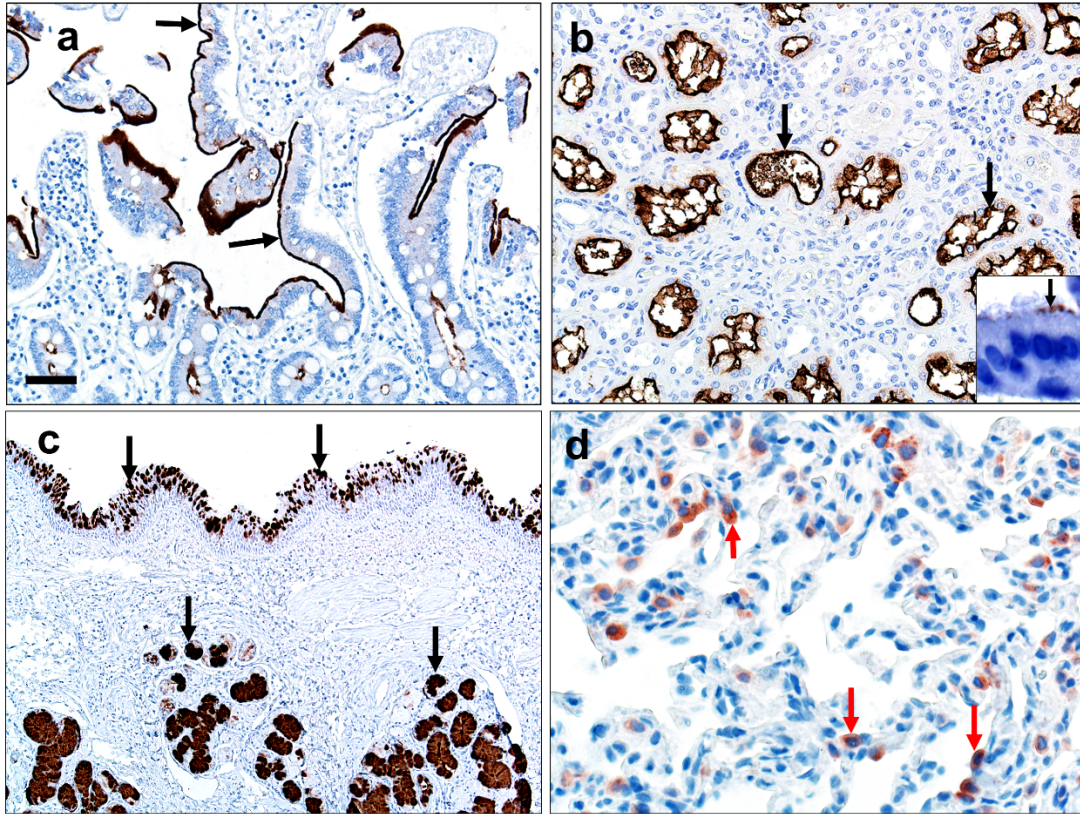


640

641 **Supplemental Figure 3.** Single-cell RNA sequencing reanalyses of ACE2 transcript abundance
 642 in nasal brushing (**a, b**) and nasal turbinate (**c, d**) (27). **a, c**) Uniform manifold approximation
 643 and projection (UMAP) visualizations. Cells were clustered using a shared nearest neighbor
 644 (SNN) approach. Cell types associated with each cluster were identified by determining marker
 645 genes for each cluster. Each data point denotes a cell. On the right panels, cells with ACE2
 646 transcripts are shown in red. **b, d**) Violin plots representing ACE2 expression. In nasal turbinate
 647 and nasal brushing, percentage of ACE2⁺ cells within each cell type shows ACE2 expression on
 648 epithelial cells. Each data point denotes a cell, most cells have no expression (0). DC: dendritic
 649 cells. NK: Natural killer. CPM: Counts per million.

650

Supplemental Figure 4



651

652 **Supplemental Figure 4.** Quality controls for ACE2 immunohistochemistry technique (**a, b**) and
653 tissue quality (**c, d**). **a, b**) ACE2 protein (brown color, black arrows) was detected along the
654 apical surface of small intestine enterocytes (**a**), renal tubule epithelium (**b**), and ciliated cells (**b**,
655 **inset**) of primary airway cell cultures. These findings demonstrate specific detection of ACE2
656 protein in cells/tissues consistent with known ACE2 expression. **c**) Representative
657 immunostaining of bronchus detected abundant MUC5B protein (brown color, black arrows) in
658 mucous cells of surface epithelium (top) and submucosal glands (bottom). **d**) Representative
659 sections of alveoli had SP-C⁺ alveolar type II cells (red color, red arrows). These results (**c, d**)
660 demonstrate the tissues were intact and that immunostaining can be used to detect native airway
661 (**c**) and lung (**d**) proteins. Bar = 40 (a, b), 80 (c), and 20 μ m (d).

666 **Supplemental Table 1. ACE2 protein reported in surface epithelium (SE) of human**
 667 **respiratory tract surface epithelium.**

Reported Cases [n]	Primary Ab	SN	T	B	Br	Al	Summary comments
Non-diseased lungs / nasal [5 each]; diseased lungs [5] (20)	Polyclonal	SE (C++, basal cells in squamous epithelium)	n.d.	SE (C+)	n.d.	AT1 (C++); AT2 (C++)	Abundant ACE2 protein in lung epithelia
Non-diseased lungs [5] (21)	Undefined	n.d.	SE (C+, A+)	SE (C+, A+)	n.d.	"Alveoli" (A+) Mac (A+)	ACE2 is present on epithelia in several parts of the respiratory tract and macrophages
Lung [undefined] (22)	Polyclonal	n.d.	n.d.	SE (C+, N+, M+)	n.d.	AT1- AT2 (N+)	ACE2 is present in bronchial epithelium, AT2 cells, and macrophages
Sinus [undefined] and Lung [undefined, same tissues as above] (23)	Polyclonal	SE (N++)	SE (-)	SE (C+, N++)	n.d.	AT1- AT2 (N++)	ACE2 is present in sinus and bronchial epithelium, AT2 cells, and macrophages

668

669 Non-diseased: The cause of death was not directly related to lung disease

670 n.d.: Not described

671 Tissues: Sinonasal (SN), trachea (T), bronchi (B), bronchioles (Br), and alveoli (Al)

672 Cellular localization: cytoplasmic (C), nuclear (N), apical membrane (A)

673 Cells: Surface epithelium (SE), alveolar type I cells (AT1), alveolar type II cells (AT2), alveolar

674 macrophages (Mac)

675 ACE2 protein (based on published reports/figures): negative (-), weak (+), moderate to abundant

676 (++)

677 **Supplemental Table 2. Donor demographics and ACE2 distribution scores for each tissue**
 678 **region.**

Case #	Group	Age (yrs)	Sex	Comorbidities	Trachea	Bronchi	Bronchioles	Alveoli
1	Control	5	F	Trauma	NA	2	2	1
2	Control	57	M	Arrhythmia	0	0	0	1
3	Control	31	M	Stroke (Joubert syndrome)	1	1	0	0
4	Control	53	F	Trauma	NA	0	0	1
5	Control	2	M	Brain hemorrhage	0	0	0	1
6	Control	2	M	Trauma	0	0	1	2
7	Control	0-5	M	Spinomuscular atrophy	NA	0	1	0
8	Control	71	M	Stroke, Parkinson's disease, nonsmoker	0	1	1	0
9	Control	4	F	Trauma	0	0	0	2
10	Control	1-2	M	Trauma	0	NA	1	1
11	Control	53	F	Trauma, nonsmoker	0	0	2	0
12	Control	26	F	NA	0	NA	0	0
13	Control	27	F	NA	NA	0	1	0
14	Control	64	M	NA	NA	1	1	0
15	Chronic disease	53	F	Smoker	0	NA	0	1
16	Chronic disease	60	M	COPD, smoker	NA	NA	0	1
17	Chronic disease	32	M	COPD, smoker	0	0	0	1
18	Chronic disease	68	M	COPD	NA	1	0	1
19	Chronic disease	68	F	COPD	NA	NA	1	1
20	Chronic disease	9	M	Asthma	0	0	0	1
21	Chronic disease	25	F	Cystic fibrosis	NA	0	0	0
22	Chronic disease	47	F	Cardiovascular disease	1	2	2	1
23	Chronic disease	27	M	Cystic fibrosis	0	NA	NA	1
24	Chronic disease	50	F	Cardiovascular disease, diabetes, asthma	NA	0	0	0
25	Chronic disease	37	M	Drug use, smoker	0	0	0	0
26	Chronic disease	38	M	Asthma (status asthmaticus)	0	0	0	0
27	Chronic disease	32	M	Cystic fibrosis	NA	NA	0	1
28	Chronic disease	58	F	Cardiovascular disease, diabetes, NASH	0	0	0	1
29	Chronic disease	19	F	Cystic fibrosis	NA	0	0	0

679

680 NA: Not available for analyses / COPD: Chronic obstructive pulmonary disease / NASH: Non-
 681 alcoholic steatohepatitis.

682 Scoring: 0 = below limit of immunohistochemical detection; 1 = rare (<1%); 2 = 1-33%; 3 = 34-
 683 66%; 4 = >66% of cells.

684

685 **Supplemental Table 3. Parameters for immunohistochemistry on fixed tissues.**

Target	Primary Antibody	Antigen Retrieval	Secondary Reagents
Angiotensin- Converting Enzyme 2 (ACE2)	Anti-ACE2, monoclonal (MAB933, R&D Systems, Minneapolis, MN USA) in diluent at 1:100 x 1 hour.	HIER, Citrate Buffer, pH 6.0, 110°C for 15 minutes; 20 min cool down (Decloaking Chamber Plus, Biocare Medical, Concord, CA USA)	Dako EnVision+ System- HRP Labeled Polymer Anti-mouse, 60 min (Dako North America, Inc., Carpentaria, CA USA), DAB Chromogen, counterstain.
MUC5B	Rabbit anti-MUC5B polyclonal, (LSBio #LS-B8121, LifeSpan BioSciences, Inc., Seattle, WA) in Dako Antibody Diluent (Dako North America, Inc., Carpentaria, CA); 1:60,000/30 min	HIER, Citrate buffer pH 6.0, 110°C for 15min; 20 min cool down	Step 1: Biotinylated anti- Rabbit IgG (H+L) (Vector Laboratories, Inc., Burlingame, CA) in Dako Wash Buffer (Dako North America, Inc., Carpentaria, CA); 1:500, 30 min Step 2: Vectastain ABC Kit (Vector Laboratories, Inc., Burlingame, CA), 30min. DAB Chromogen, counterstain.
Surfactant Protein – C (SP-C)	Anti-SP-C, polyclonal (PA5-71680, Thermo Fisher Scientific, Waltham, MA USA) in diluent 1:100 x 1 hour	HIER, Citrate Buffer, pH 6.0, 110°C for 15 minutes; 20 min cool down (Decloaking Chamber Plus, Biocare Medical, Concord, CA USA)	Dako EnVision+ System- HRP Labeled Polymer Anti-rabbit, 60 min (Dako North America, Inc., Carpentaria, CA USA), AEC chromogen, counterstain.

686

687 HIER – Heat-induced epitope retrieval

688 DAB – 3,3'-Diaminobenzidine (produces brown stain)

689 AEC - aminoethyl carbazole (produces red stain)

690 Counterstain – Harris hematoxylin (blue color)